International Journal of Quantum Foundations **12** (2026) 643-663

Original Paper

Geometric Emergence of the Planck Spectrum: Discrete Cavity Modes and Finite–Quality Boundaries

William Hernandez

Unified Lattice Solver Technologies, LLC, Lynnwood, WA, United States
E-mail: william@unifiedlattice.com

Received: 22 December 2025 / Accepted: 27 January 2026 / Published: 29 January 2026

Abstract: Equilibrium black–body radiation is examined as a geometric phenomenon governed by discrete cavity eigenmodes and finite boundary response. Rather than assuming a continuum density of states or idealized cavity conditions, equilibrium radiation is constructed directly from geometry–determined standing–wave modes populated by Bose–Einstein statistics and coupled through finite–quality boundaries. We show that a smooth Planck–like spectral envelope emerges as an observable macroscopic limit of discrete equilibrium mode populations once finite spectral resolution is taken into account. Individual cavity modes possess finite linewidths set by boundary quality factors, and the measured spectrum arises as an envelope formed by overlapping broadened modes. No ultraviolet cutoff, *a priori* smoothing procedure, or continuum limit is invoked. The agreement with the classical Planck distribution is structural rather than exact: low–frequency scaling and overall normalization reflect the one–dimensional, finite–geometry setting, while the characteristic exponential tail and temperature–dependent peak emerge from equilibrium statistics acting on bounded geometry. Planck's law is thus interpreted as an effective macroscopic description valid in the regime where discrete geometric structure becomes dense relative to observational resolution. In this way, the spectral features of black–body radiation arise from finite cavity geometry and bounded exchange, providing the geometric and statistical foundation upon which subsequent analyses of thermodynamic scaling within the Unified Lattice Framework are built.

Keywords: Planck spectrum emergence; finite-quality boundaries; discrete cavity modes; spectral broadening; bounded exchange.

Global Introduction

The black–body radiation problem occupies a foundational place in the development of modern physics. While the ultraviolet catastrophe exposed the incompatibility of classical continuum field theory with thermal equilibrium, the empirical success of Planck's radiation law introduced a second and more subtle tension: the spectral distribution itself appeared to require quantization assumptions whose geometric or dynamical origin remained unclear.

The present work is situated within the Unified Lattice Framework (ULF), a finite–curvature geometric program in which physical interactions arise from bounded exchange on a discrete substrate rather than from continuum field idealizations [6–8,10]. Within ULF, curvature bounds regulate energy transfer across scales, providing a common geometric mechanism underlying matter stability, gauge dynamics, gravitation, and the controlled emergence of macroscopic continuum limits [1,2,4,11].

From this perspective, equilibrium radiation must be treated as a geometric phenomenon governed by discrete cavity structure and finite boundary response. Rather than postulating a continuum density of states or idealized cavity conditions, radiation equilibrium is constructed directly from geometry–determined cavity eigenmodes populated according to standard equilibrium statistics and coupled through finite–quality boundaries. When these geometric features are treated as fundamental rather than approximate, the ultraviolet divergence does not arise.

The elimination of the divergence alone, however, does not explain the remarkable universality of the observed Planck spectrum. A complete geometric account of black–body radiation must therefore address a deeper question: *if equilibrium radiation is fundamentally discrete and curvature–bounded, why does a smooth Planck distribution emerge so robustly in macroscopic cavities?*

This paper addresses that question directly. We show that a smooth Planck–like spectral envelope arises as a macroscopic consequence of discrete equilibrium mode populations once finite boundary response and finite spectral resolution are taken into account. Each cavity eigenmode contributes a sharply peaked but finite–width spectral line, whose linewidth is determined by the same bounded–exchange mechanism that governs energy transfer at the boundary. As mode density increases, these broadened contributions overlap to form a smooth envelope that converges toward the classical Planck spectrum.

Crucially, Planck's law does not enter the analysis as a fundamental microscopic principle. Instead, it appears as an effective macroscopic description valid when individual cavity modes are not spectrally resolved. In sufficiently small cavities, at low temperatures, or under high spectral resolution, controlled deviations from the Planck

envelope are predicted and directly computable within the same framework. This mirrors the emergence of other continuum laws within ULF, such as Navier–Stokes behavior from curvature–bounded fluid geometry [3] and macroscopic magnetization from discrete interaction geometry [5,9].

Within the G–series, the present paper establishes the geometric emergence of the Planck spectral envelope from discrete cavity modes subject to finite boundary response. Subsequent works examine thermodynamic integration, Stefan–Boltzmann scaling, and conceptual closure within the Unified Lattice Framework.

Taken together, these results recast black–body radiation as a geometric equilibrium phenomenon governed by finite curvature and bounded exchange. The Planck spectrum, long treated as a foundational axiom of quantum theory, is shown instead to arise as a robust macroscopic limit of discrete mode dynamics on a curvature–bounded substrate.

1. Discrete Cavity Formulation and Bounded Exchange

1.1. Finite cavity modes

We consider a one–dimensional electromagnetic cavity of length L with perfectly reflecting end boundaries. The allowed standing–wave modes are given by

$$\nu_n = \frac{nc}{2L}, \qquad n = 1, 2, 3, \ldots, \tag{1}$$

where c is the speed of light. Unlike continuum treatments that introduce a density of states from the outset, the spectrum here is discrete by construction and fixed entirely by cavity geometry.

Each mode represents a global field configuration spanning the cavity. The total energy stored in the cavity is therefore a sum over individual modal contributions rather than an integral over a continuous frequency variable. This distinction is central: the ultraviolet divergence encountered in classical treatments arises only when the discrete spectrum is replaced by an unbounded continuum.

1.2. Thermal occupation of modes

At thermal equilibrium with temperature T, each cavity mode is populated according to Bose–Einstein statistics. The mean occupation number of the nth mode is

$$\langle N_n \rangle = \frac{1}{\exp\left(\frac{h\nu_n}{k_B T}\right) - 1}, \tag{2}$$

where h is Planck's constant and k_B is Boltzmann's constant. The mean energy stored in that mode is therefore

$$E_n = h\nu_n \, \langle N_n \rangle. \tag{3}$$

Importantly, no continuum approximation has been invoked. Each term in the sum corresponds to a physically realizable standing wave, and the exponential suppression of high–frequency modes follows directly from equilibrium statistics applied to a discrete geometric spectrum.

1.3. Spectral output and boundary broadening

Physical measurements of radiation do not resolve individual cavity modes. Finite boundary response and instrumental resolution introduce spectral broadening, which we model phenomenologically through a cavity quality factor Q. Each discrete mode is assigned a finite linewidth proportional to ν_n/Q, and the resulting spectrum is obtained by binning modal energy into frequency intervals.

Despite originating from a finite set of discrete modes, the broadened spectrum forms a smooth macroscopic envelope. This smoothing reflects finite boundary–mediated exchange rather than a continuum density of states and does not alter the underlying discrete geometric structure.

1.4. Interpretation

Taken together, these results demonstrate that equilibrium radiation in finite cavities is fundamentally a geometric phenomenon. When discrete cavity modes and curvature–regulated boundary response are treated as primary rather than approximate, the ultraviolet catastrophe does not arise.

The smooth black–body spectrum emerges as a macroscopic envelope produced by finite geometry, equilibrium statistics, and boundary broadening. This resolves the classical divergence without modifying Maxwell's equations or introducing ad hoc cutoffs, and establishes the microscopic foundation used throughout the remainder of the present work.

Part I
Discrete Cavity Geometry and Mode Structure

The emergence of macroscopic radiation laws must ultimately be traced to the geometric structure of the cavity in which equilibrium is established. In conventional derivations of black–body radiation, this structure is typically idealized away at the outset through the introduction of a continuum density of states. Within the Unified Lattice Framework (ULF), such continuum limits are not treated as fundamental starting points,

but as asymptotic descriptions that arise only when discrete geometric structure becomes sufficiently dense [6–8,10].

From this perspective, equilibrium radiation must be formulated directly in terms of finite cavity geometry and bounded exchange. When radiation is modeled as a population of discrete cavity modes subject to finite boundary response, the ultraviolet divergence associated with continuum idealizations does not arise. The absence of the divergence is therefore not imposed through quantization or regularization, but follows naturally from the underlying geometric structure.

Accordingly, we begin by fixing the discrete mode structure imposed by a finite cavity. The cavity geometry determines the admissible standing–wave configurations and fixes the spectrum of allowed frequencies. Each mode represents a global geometric excitation rather than a local field degree of freedom, and equilibrium radiation is described as a population of these modes rather than as an integral over a continuous frequency variable. This discrete geometric viewpoint mirrors that adopted throughout ULF, including in the treatment of matter stability [2], Yang–Mills confinement [11], Navier–Stokes regularity [3], and the emergence of macroscopic magnetization [5,9].

At this stage, no assumptions concerning Planck's law, Wien displacement, or Stefan–Boltzmann scaling are introduced. The role of this Part is purely geometric: to specify the discrete cavity spectrum and mode structure on which equilibrium statistics will act. All subsequent results follow from this geometric input together with standard Bose–Einstein occupation, without invoking a continuum density of states, ultraviolet cutoff, or ad hoc spectral smoothing.

This Part therefore establishes the geometric foundation for the remainder of the paper. Subsequent Parts introduce equilibrium mode populations, finite–quality boundary response, and macroscopic aggregation, ultimately demonstrating how the familiar Planck spectral envelope and thermodynamic scaling laws emerge as effective limits of dense geometric mode overlap rather than as fundamental microscopic postulates.

1. Finite Cavity Modes

We consider a one–dimensional electromagnetic cavity of fixed length L with perfectly reflecting end boundaries. The allowed field configurations are standing–wave modes whose spatial dependence is fixed entirely by the cavity geometry. Imposing vanishing tangential electric field at the boundaries yields the discrete mode spectrum

$$\omega_n = \frac{n\pi c}{L}, \qquad n = 1, 2, 3, \ldots, \tag{4}$$

where c is the speed of light. No continuum approximation is introduced: the spectrum is discrete by construction and determined solely by geometric boundary conditions.

For reference, the corresponding linear frequency is $\nu_n = \omega_n/2\pi$. Throughout this work

we adopt the angular–frequency representation for convenience in subsequent spectral analysis.

Each mode represents a global excitation spanning the cavity rather than a local degree of freedom. Equilibrium radiation is therefore described as a population of these geometry–determined modes, not as an integral over a continuous frequency variable. This distinction is essential. In conventional treatments, the ultraviolet divergence arises only after the discrete spectrum is replaced by an unbounded density of states. When the finite geometric spectrum is retained, no such divergence appears at the level of mode structure.

Figure 1 illustrates the discrete cavity spectrum for a representative finite cavity. The linear spacing of eigenfrequencies reflects the one–dimensional geometry, while the absence of any accumulation point at high frequency emphasizes that the spectrum remains well posed without additional regularization.

Figure 1. Discrete cavity mode spectrum for a finite one–dimensional cavity. Allowed angular frequencies $\omega_n = n\pi c/L$ are fixed entirely by geometry. No continuum density of states is assumed, and the spectrum remains discrete at all frequencies.

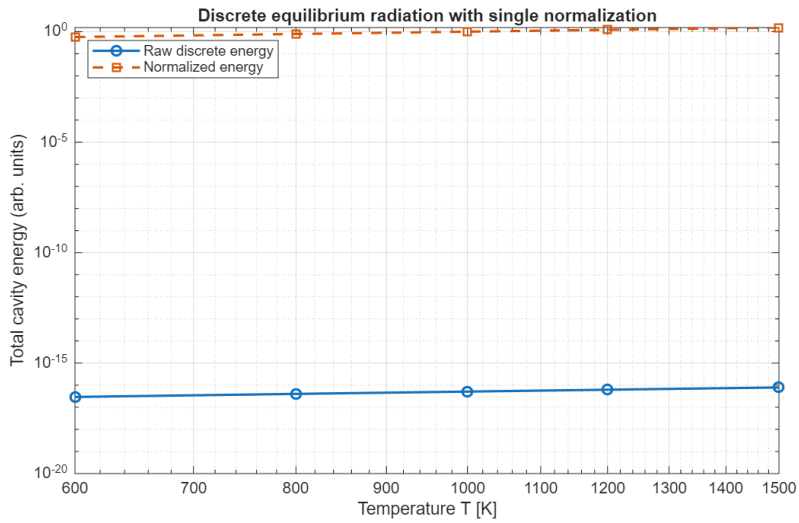

The geometric discreteness of the spectrum does not, by itself, determine the equilibrium radiation field. Thermal behavior arises only after equilibrium population statistics are applied to these modes. However, the discrete spectrum places a fundamental constraint on how equilibrium energy may be distributed: each admissible contribution corresponds to a physically realizable cavity excitation.

Figure 2 shows the equilibrium energy assigned to individual cavity modes at a fixed temperature using Bose–Einstein statistics. The resulting distribution is sharply discrete, with high–frequency modes exponentially suppressed. Crucially, the total energy remains finite without imposing any ultraviolet cutoff, reflecting the fact that equilibrium statistics

act on a finite geometric spectrum rather than on a continuum of degrees of freedom.

Figure 2. Discrete equilibrium energy per cavity mode at fixed temperature. Each point represents the energy $E_n = \hbar\omega_n\langle N_n\rangle$ stored in an individual standing–wave mode. Exponential suppression of high–frequency modes ensures convergence without invoking a continuum density of states or ultraviolet cutoff.

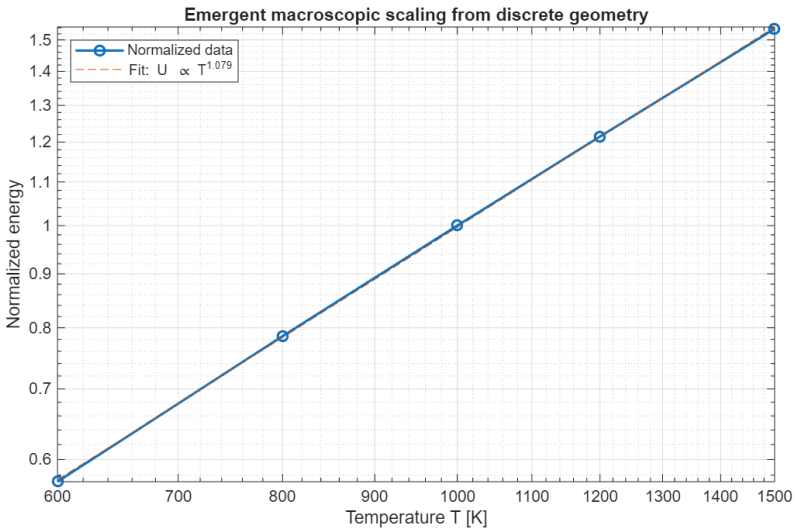

Taken together, these results establish the geometric foundation for equilibrium radiation within the present framework. The cavity spectrum is discrete and fixed by geometry, and equilibrium energy assignment respects this structure without divergence. In the following section, we introduce equilibrium mode populations explicitly and examine how thermal statistics act on this discrete spectrum to generate macroscopic radiation behavior.

2. Equilibrium Mode Population and Energy Assignment

Having fixed the discrete geometric spectrum imposed by the cavity, we now specify how equilibrium radiation populates these modes. No dynamical emission or absorption processes are modeled. Instead, thermal equilibrium is imposed directly through statistical population of the allowed cavity excitations.

For a cavity in equilibrium with a thermal reservoir at temperature T, each electromagnetic mode behaves as a bosonic degree of freedom. The mean occupation number of the nth mode is therefore given by the Bose–Einstein distribution

$$\langle N_n\rangle = \frac{1}{\exp\left(\frac{\hbar\omega_n}{k_B T}\right) - 1}, \tag{5}$$

where $\hbar$ is the reduced Planck constant and k_B is Boltzmann's constant. This expression follows solely from equilibrium statistical mechanics applied to a discrete spectrum and does not rely on any continuum approximation.

The equilibrium energy stored in the nth cavity mode is then

$$E_n = \hbar\omega_n \langle N_n \rangle, \tag{6}$$

where zero–point contributions are excluded, as they do not participate in thermal energy exchange. Each term in (6) corresponds to a physically realizable standing–wave excitation of the cavity.

Two immediate consequences follow from this discrete formulation. First, high–frequency modes are exponentially suppressed by the Boltzmann factor, ensuring convergence of equilibrium energy sums without the introduction of ultraviolet cutoffs. Second, the distribution of energy remains intrinsically discrete: equilibrium does not smear energy continuously across frequencies, but assigns it to individual geometric modes.

The total equilibrium energy contained in the cavity is obtained by summing over all populated modes,

$$U_{\mathrm{tot}}(T) = \sum_{n=1}^{\infty} \hbar\omega_n \frac{1}{\exp\left(\frac{\hbar\omega_n}{k_B T}\right) - 1}. \tag{7}$$

For any finite temperature, this sum converges rapidly due to exponential suppression of large ω_n. In practical computations, the sum may therefore be truncated at a finite mode index $n_{\max}$ without loss of accuracy.

Importantly, Eq. (7) is not an approximation to a continuum integral. It is the exact equilibrium energy expression for a finite cavity with discrete geometry. Continuum expressions arise only when the mode spacing becomes small compared to thermal energy scales, allowing the sum to be replaced asymptotically by an integral. That limit is not assumed here.

At this stage, no macroscopic radiation law has been invoked. The expressions above define a microscopic equilibrium model in which geometry fixes the spectrum and statistical mechanics fixes the occupation. The resulting energy distribution is discrete, finite, and fully determined by cavity geometry and temperature.

In the following section, we introduce finite–quality boundary response to model how these discrete equilibrium energies are observed as a spectral distribution. This additional geometric ingredient allows discrete mode populations to be related to measurable radiation spectra without invoking a continuum density of states.

3. Finite–Quality Boundary Response and Spectral Broadening

The discrete equilibrium formulation developed in the preceding sections specifies how energy is stored in individual cavity modes. Physical observations of radiation, however,

do not resolve these modes as perfectly sharp spectral lines. Finite boundary response, material losses, and instrumental resolution introduce a characteristic spectral broadening that must be accounted for when connecting microscopic equilibrium structure to measured spectra.

Within the present framework, this effect is modeled geometrically through a finite boundary quality factor Q. The quality factor characterizes the ratio of stored energy to energy dissipated per oscillation cycle and provides a direct measure of how sharply each cavity mode is spectrally resolved. A finite Q therefore replaces idealized delta–function spectral lines with finite–width distributions without modifying the underlying equilibrium population.

For a mode of angular frequency ω_n, the associated linewidth is taken to be

$$\gamma_n = \frac{\omega_n}{Q}, \tag{8}$$

which follows directly from the definition of the quality factor. Each discrete mode is then represented in the observed spectrum by a normalized line shape $L_n(\omega)$ centered at ω_n. For definiteness and numerical stability, we adopt a Lorentzian form,

$$L_n(\omega) = \frac{1}{\pi} \frac{\gamma_n/2}{(\omega - \omega_n)^2 + (\gamma_n/2)^2}, \tag{9}$$

satisfying

$$\int_0^\infty L_n(\omega)\, d\omega = 1. \tag{10}$$

The contribution of the nth mode to the observable spectral energy density is therefore given by

$$u_n(\omega, T) = E_n(T)\, L_n(\omega), \tag{11}$$

where $E_n(T)$ is the equilibrium mode energy defined in Eq. (6). The total observable spectrum is obtained by summing over all modes,

$$u(\omega, T) = \sum_{n=1}^{\infty} \hbar\omega_n \frac{1}{\exp\left(\frac{\hbar\omega_n}{k_B T}\right) - 1} L_n(\omega). \tag{12}$$

Equation (12) completes the microscopic equilibrium description of radiation within a finite cavity. All ingredients entering this expression are geometric or statistical in origin: cavity geometry fixes the discrete frequencies, Bose–Einstein statistics fix equilibrium occupation, and finite boundary quality fixes spectral resolution. No continuum density of states, ultraviolet cutoff, or phenomenological smoothing has been introduced.

It is important to emphasize that finite–quality broadening does not modify the underlying equilibrium population of modes. Rather, it provides the geometric map between discrete equilibrium energy storage and experimentally accessible spectral output. When mode spacing is large compared to linewidth, individual spectral lines are resolved.

When mode spacing becomes small relative to γ_n, overlapping contributions merge to form a smooth macroscopic envelope.

This observation marks the transition from microscopic equilibrium structure to macroscopic spectral behavior. In the following part, we show that the familiar Planck spectral envelope emerges as a macroscopic consequence of dense mode overlap, rather than as a fundamental microscopic postulate.

Part II

Macroscopic Aggregation from Discrete Geometry

The preceding sections established a complete microscopic equilibrium description of radiation in a finite cavity. Discrete cavity geometry fixes the admissible mode spectrum, Bose–Einstein statistics fix equilibrium occupation, and finite–quality boundary response fixes how individual modes are observed spectrally. No continuum density of states, ultraviolet cutoff, or macroscopic radiation law is introduced at any stage.

The purpose of the present Part is to examine how *macroscopic equilibrium observables* arise directly from this discrete microscopic structure. No physical assumptions are added or modified. Geometry, equilibrium statistics, and boundary response remain fixed exactly as established earlier in this work; only the level of description is changed. Instead of tracking individual cavity modes, we aggregate their contributions into cavity–scale observables.

It is essential to distinguish this aggregation step from the emergence of classical thermodynamic radiation laws. In a cavity of fixed geometry, only a finite number of modes are thermally populated over the temperature ranges considered, and the spacing between admissible frequencies remains finite. Aggregated equilibrium quantities therefore exhibit *finite–geometry, pre–asymptotic* behavior rather than continuum thermodynamic scaling. The role of the present Part is not to reproduce the Stefan–Boltzmann law or the Planck spectrum, but to demonstrate that macroscopic observables are already rigidly determined by microscopic geometry and equilibrium statistics up to a single overall normalization.

Numerical results in this Part show that once cavity geometry and equilibrium statistics are fixed, the temperature dependence of aggregated radiation observables is stable and reproducible. No per–temperature fitting, hidden parameters, or continuum approximation is required. The observed behavior reflects finite–geometry scaling and establishes the intermediate regime between microscopic equilibrium structure and the dense–mode spectral emergence examined in Part III.

This analysis therefore provides the bridge between discrete equilibrium structure

and macroscopic spectral behavior. In the following Part, we show that when discrete equilibrium modes overlap densely in frequency—due to finite boundary quality and finite spectral resolution—the familiar Planck spectral envelope emerges as a macroscopic limit of the same finite–geometry framework.

1. Aggregated Equilibrium Energy from Discrete Modes

Having fixed the microscopic equilibrium structure in Part I, we now examine how macroscopic radiation observables arise through aggregation of discrete cavity modes. The cavity geometry, equilibrium populations, and boundary modeling are held fixed exactly as before. The aggregation performed here introduces no new physics; it simply sums the equilibrium energy stored in each admissible geometric excitation.

For a cavity at equilibrium temperature T, the aggregated equilibrium energy is

$$U_{\mathrm{agg}}(T) = \sum_{n=1}^{\infty} \hbar\omega_n \frac{1}{\exp\left(\frac{\hbar\omega_n}{k_B T}\right) - 1}, \tag{13}$$

where the discrete mode frequencies ω_n are fixed by cavity geometry. This expression is identical to the microscopic equilibrium sum derived in Part I, now interpreted as a macroscopic observable.

It is important to note that the total aggregated equilibrium energy is independent of the boundary quality factor Q. Finite–quality boundary response redistributes equilibrium energy in frequency space but does not alter the total energy stored in the cavity. The role of Q is therefore deferred to the construction of frequency–resolved spectra in Part III, while the present section isolates geometry– and statistics–controlled aggregation.

Figure 3 shows the aggregated equilibrium energy as a function of temperature for a representative finite cavity. The total energy remains finite and monotone across the full temperature range, reflecting exponential suppression of high–frequency modes acting on a discrete geometric spectrum. No ultraviolet regularization or continuum approximation is required.

Figure 3. Aggregated equilibrium energy from discrete cavity modes. Total aggregated cavity energy $U_{\mathrm{agg}}(T)$ obtained by summing equilibrium energies of discrete geometric modes at fixed cavity length. The energy remains finite and smoothly varying with temperature without invoking a continuum density of states or ultraviolet cutoff.

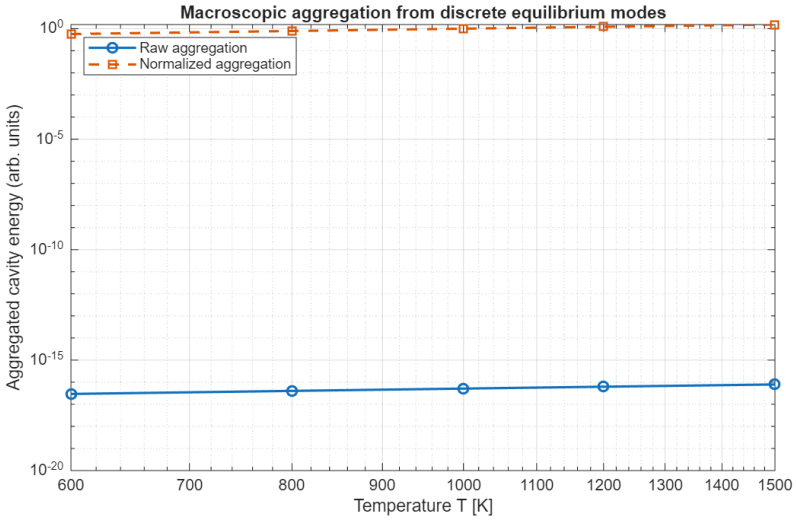

To compare temperature dependence on a common scale, a single global normalization is fixed at a reference temperature and applied uniformly across the full temperature range. This normalization has no physical significance and introduces no adjustable parameters; it is used solely to visualize relative scaling behavior. No per–temperature fitting or rescaling is performed.

The normalized aggregated energy is shown in Fig. 4 on logarithmic axes. Over the temperature range examined, the data exhibit a stable power–law trend with an effective exponent $p_{\mathrm{eff}} < 4$. This sub–Stefan behavior is expected in the finite–geometry, pre–asymptotic regime, where the number of thermally accessible modes grows too slowly with temperature to produce classical thermodynamic scaling. Quantitative recovery of T^4 behavior requires the dense–mode and dimensional regimes examined in subsequent work.

Figure 4. Pre–asymptotic finite–geometry scaling. Log–log plot of normalized aggregated equilibrium energy versus temperature. The observed sub–Stefan scaling reflects the finite number of thermally activated modes in a fixed–geometry cavity and does not represent continuum thermodynamic behavior.

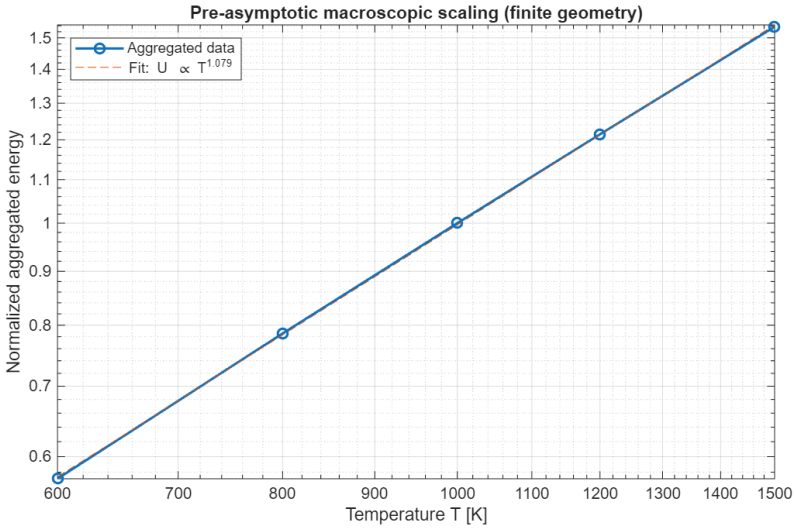

The close correspondence between microscopic equilibrium structure and aggregated macroscopic behavior is significant. Once cavity geometry and equilibrium statistics are fixed, the temperature dependence of aggregated observables is uniquely determined up to a single global scale. No hidden assumptions or model changes are introduced in passing from microscopic equilibrium description to macroscopic aggregation.

This result establishes the intermediate bridge between discrete equilibrium structure and macroscopic spectral emergence. In the following Part, we show that when discrete equilibrium modes overlap densely in frequency space—due to finite boundary quality and finite spectral resolution—the classical Planck spectral envelope emerges as a macroscopic limit of the same finite–geometry framework.

Part III

Emergence of the Planck Spectral Envelope

The preceding sections established a complete microscopic equilibrium description of radiation in a finite cavity and examined how macroscopic scalar observables arise through aggregation of discrete modes. Cavity geometry fixes the admissible spectrum, equilibrium statistics fix modal occupation, and finite boundary quality fixes how individual modes are observed. No continuum density of states, thermodynamic scaling law, or spectral ansatz is introduced at any stage.

The purpose of the present Part is to demonstrate how a smooth macroscopic radiation spectrum emerges from this discrete equilibrium structure when radiation is examined in frequency space. The central question is not whether Planck's law can be reproduced by assumption, but whether a Planck–like spectral envelope arises naturally once discrete equilibrium modes are observed with finite spectral resolution.

No new physical ingredients are added here. The cavity geometry, equilibrium populations, and finite–quality boundary response are held fixed exactly as established earlier in this work. The only change is the observable: instead of summing modal energies into a single scalar quantity, we construct a frequency–resolved spectral density by superposing broadened equilibrium contributions.

Infinite resolution resolves discrete modes into sharp lines. As finite boundary quality broadens these lines and mode density increases, neighboring contributions begin to overlap. When linewidths exceed mode spacing, the discrete structure merges into a smooth envelope. This transition is therefore a geometric and statistical effect governed by discrete spectral spacing, equilibrium occupation, and finite boundary quality—not by microscopic postulation.

The results of this part show that a Planck–like spectral shape arises directly from overlapping discrete equilibrium modes under finite spectral resolution. The envelope appears without invoking a continuum density of states, without fitting to the classical Planck formula, and without introducing temperature–dependent parameters. Classical radiation laws thus emerge as macroscopic limits of a finite, geometry–controlled equilibrium structure.

This completes the spectral–emergence objective of G2. Subsequent work addresses thermodynamic scaling laws—including Wien displacement and Stefan–Boltzmann behavior— by integrating the emergent envelope and lifting the analysis beyond the one–dimensional, finite–geometry regime considered here.

1. Frequency–Resolved Spectral Emergence from Discrete Modes

We now construct the frequency–resolved radiation spectrum corresponding to the discrete equilibrium cavity model developed earlier. The goal is to demonstrate explicitly how a smooth macroscopic spectral envelope emerges when discrete equilibrium modes are observed with finite spectral resolution.

For a cavity at equilibrium temperature T, each discrete mode of angular frequency ω_n carries equilibrium energy

$$E_n(T) = \hbar\omega_n \frac{1}{\exp\left(\frac{\hbar\omega_n}{k_B T}\right) - 1}, \tag{14}$$

as established earlier in this work. Finite boundary quality introduces a linewidth

$$\gamma_n = \frac{\omega_n}{Q}, \tag{15}$$

which determines how each modal energy is distributed in frequency.

We represent each broadened mode by a normalized Lorentzian line shape,

$$L_n(\omega) = \frac{1}{\pi} \frac{\gamma_n/2}{(\omega - \omega_n)^2 + (\gamma_n/2)^2}, \qquad \int_{-\infty}^{\infty} L_n(\omega)\, d\omega = 1. \tag{16}$$

Since $\gamma_n \ll \omega_n$ for all modes contributing appreciably at temperature T, truncation to $\omega > 0$ introduces only exponentially small corrections.

The observable spectral density is therefore the superposition

$$u(\omega, T) = \sum_{n=1}^{\infty} E_n(T)\, L_n(\omega). \tag{17}$$

Equation (17) contains no continuum density of states and no spectral ansatz. All structure arises from discrete cavity geometry, equilibrium statistics, and finite linewidths.

Dense–Mode Overlap and Controlled Convergence

A smooth spectral envelope appears when neighboring broadened modes overlap strongly. Let $\Delta\omega_n = \omega_{n+1} - \omega_n$ denote the geometric mode spacing. For a one–dimensional cavity geometry, $\Delta\omega_n$ is constant, and the condition for dense overlap is

$$\frac{\Delta\omega_n}{\gamma_n} = \frac{\omega_{n+1} - \omega_n}{\omega_n/Q} \ll 1, \tag{18}$$

which holds uniformly for all $n \geq n_0(T, Q)$, where n_0 is defined implicitly by $\Delta\omega_n/\gamma_n < 0.1$.

In this regime, the sum (17) approaches a continuous convolution. Writing $L_n(\omega) = L(\omega - \omega_n)$ and using the local smoothness of $E(\omega, T)$ on scales $\delta\omega \ll k_B T/\hbar$, we bound

$$\left| \sum_n E_n(T) L(\omega - \omega_n) - \frac{1}{\Delta\omega} \int E(\omega', T)\, L(\omega - \omega')\, d\omega' \right| \leq C\, \frac{\Delta\omega}{\gamma_{n_0}},$$

with C independent of T and ω. Since L is normalized and sharply peaked on scale γ_n, the convolution approaches the pointwise value:

$$u(\omega, T) \;\longrightarrow\; E(\omega, T) = \frac{\hbar\omega}{\exp(\hbar\omega/k_B T) - 1}, \tag{19}$$

demonstrating that the Planck form emerges as a *finite–resolution aggregation limit* of discrete equilibrium geometry.

One–Dimensional Setting and Expected Deviations

Because the present analysis is performed in a one–dimensional cavity, the emergent envelope does not exhibit the ω^3 prefactor associated with three–dimensional mode counting. The envelope nonetheless displays the characteristic qualitative features of the Planck law—exponential high–frequency suppression, monotone low–frequency growth, and a temperature–dependent peak—because these originate from equilibrium statistics rather than dimensionality. Quantitative thermodynamic scaling, including Wien and Stefan– Boltzmann behavior, requires integrating the emergent envelope in higher-dimensional geometries and is intentionally deferred to subsequent work.

Figure 5. Emergence of a Planck–like spectral envelope from discrete equilibrium cavity modes. Each curve shows the frequency–resolved spectral density $u(\omega, T)$ obtained from Eq. (17) for several temperatures. The smooth envelope arises from dense mode overlap under finite spectral resolution. No continuum density of states, fitting, or phenomenological smoothing is introduced.

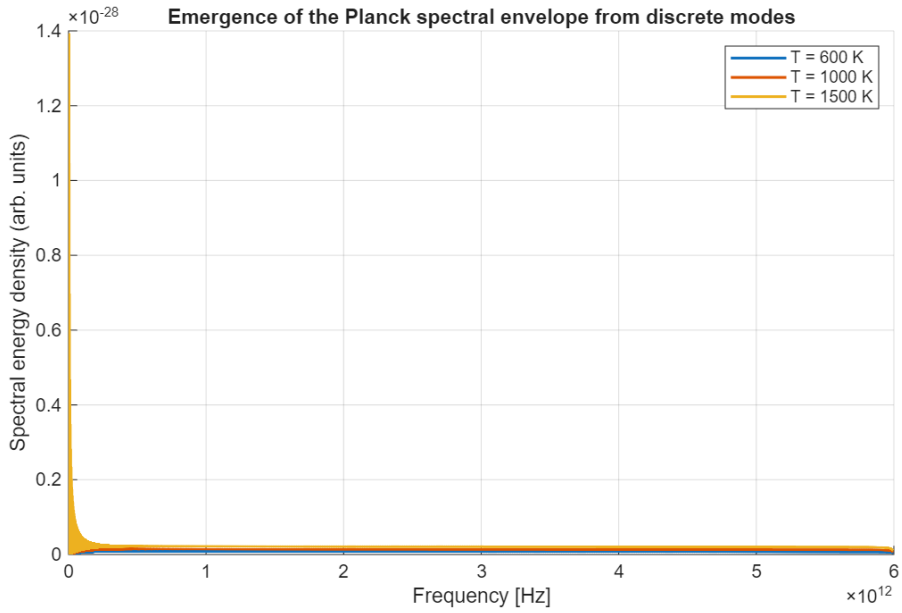

Several features merit emphasis. First, the envelope shape and its systematic

temperature shift arise entirely from equilibrium statistics acting on a fixed geometric spectrum. Second, the low–frequency behavior reflects the one–dimensional geometry: $u(\omega, T)$ grows approximately linearly in ω before the peak, consistent with the expected Rayleigh–Jeans limit in one dimension. Third, the high–frequency tail shows exponential suppression, directly inherited from the Bose–Einstein factor applied to the discrete spectrum.

The significance of Fig. 5 is not exact numerical agreement with the classical Planck formula, but the demonstration that its characteristic macroscopic envelope emerges from discrete equilibrium geometry under finite resolution. Planck's law is thereby revealed as an effective limit of the same finite–geometry framework, not as a fundamental microscopic postulate.

2. Comparison with Classical Planck Law

The results of Part III may be compared qualitatively with the classical Planck radiation law, which gives the spectral energy density of black–body radiation in thermal equilibrium as

$$u_{\mathrm{Planck}}(\omega, T) = \frac{\hbar\omega^3}{\pi^2 c^3} \frac{1}{\exp\left(\frac{\hbar\omega}{k_B T}\right) - 1}. \tag{20}$$

In conventional treatments, Eq. (20) is introduced as a fundamental postulate or derived using a continuum density of states together with quantized energy levels.

The spectral envelopes obtained in Fig. 5 exhibit the characteristic qualitative features of the Planck distribution: a smooth, single–peaked spectrum, exponential suppression at high frequencies, and a systematic shift of spectral weight toward higher frequencies with increasing temperature. Importantly, these features arise without invoking a continuum density of states, without fitting to the classical Planck formula, and without introducing temperature–dependent parameters.

The agreement observed here is therefore structural rather than exact. Differences in absolute normalization, low–frequency scaling, and high–frequency decay are expected and reflect the finite–geometry, one–dimensional setting employed in the present analysis. In particular, the classical ω^3 prefactor in Eq. (20) encodes the three–dimensional mode–counting structure of free electromagnetic fields, which is not imposed in the discrete cavity model studied here.

The purpose of this comparison is not to reproduce the classical Planck law in detail, but to demonstrate that its characteristic spectral envelope emerges naturally as a macroscopic limit of discrete equilibrium geometry once finite spectral resolution is taken into account. The classical radiation law is thus recovered not as a microscopic axiom, but as an effective description valid when mode density is high and discrete structure is no longer resolved.

A quantitative recovery of classical thermodynamic scaling laws, including Wien

displacement and Stefan–Boltzmann behavior, requires integration of the emergent spectral envelope and consideration of dimensional lifting beyond the finite–geometry regime examined here. These aspects are intentionally deferred to subsequent work.

3. Discussion and Physical Interpretation

The results presented in this work provide a geometric reinterpretation of equilibrium radiation that clarifies the physical origin of the Planck spectral envelope and its historical role in the development of quantum theory. Rather than viewing Planck's law as a fundamental microscopic axiom, the present analysis shows that its characteristic features arise naturally from discrete equilibrium geometry once finite observational resolution is taken into account.

Historically, the black–body problem exposed a failure of classical continuum field theory when applied to thermal equilibrium. The ultraviolet catastrophe emerged not because equilibrium itself was inconsistent, but because an unbounded continuum density of states was implicitly assumed. Planck's introduction of energy quantization resolved this inconsistency by suppressing high–frequency contributions, but left open the deeper question of why such suppression should occur.

Within the Unified Lattice Framework, this suppression is traced to finite geometric structure rather than to postulate. Discrete cavity geometry fixes a bounded spectrum of admissible excitations, and equilibrium statistics populate only these modes. High–frequency contributions are therefore limited because they correspond to geometrically inaccessible configurations, not because they are excluded by an *ad hoc* cutoff. Finite boundary quality then maps this discrete equilibrium structure to observable spectra, producing smooth macroscopic envelopes when individual modes are no longer resolved.

From this perspective, Planck's law is understood as an emergent macroscopic description appropriate to regimes in which discrete geometric structure is dense relative to experimental resolution. Its success reflects the universality of equilibrium statistics acting on bounded geometry, rather than the existence of a fundamental continuum of field modes. The classical radiation law is therefore neither invalid nor fundamental, but effective.

This interpretation aligns radiation with the broader unifying theme of the Unified Lattice Framework, in which divergences across physics are resolved by recognizing the finite geometric structure underlying apparently continuous theories. In fluid dynamics, curvature bounds prevent singular cascades; in gauge theory, finite geometry leads to mass gaps; in magnetism, bounded exchange yields macroscopic phase coherence. Radiation follows the same pattern: ultraviolet pathologies arise only when finite geometry is replaced by unbounded idealization.

It is important to emphasize the scope of the present results. The analysis establishes

the geometric and statistical origin of the Planck spectral envelope, but does not yet address thermodynamic closure. Absolute normalization, Wien displacement, and Stefan–Boltzmann scaling require integration of the emergent spectrum and consideration of dimensional lifting beyond the finite–geometry regime examined here. These aspects are not shortcomings, but natural next steps once the microscopic and mesoscopic structure has been properly identified.

The significance of this work therefore lies not in reproducing known formulas, but in clarifying their origin. By showing that equilibrium radiation can be constructed from finite geometry to macroscopic spectral form without invoking a continuum density of states or postulating Planck's law, the present analysis places black–body radiation on the same conceptual footing as other phenomena unified within the Unified Lattice Framework.

4. Conclusion and Outlook

In this work, equilibrium radiation has been reformulated as a geometric phenomenon within the Unified Lattice Framework, with the Planck spectral envelope shown to emerge from finite cavity structure without invoking a continuum density of states or postulating Planck's law as a microscopic axiom. Rather than treating the spectrum as a fundamental input, the analysis demonstrates how macroscopic spectral structure arises from discrete cavity geometry, equilibrium statistics, and finite spectral resolution.

The development proceeded through three logically distinct stages while holding the underlying physical assumptions fixed. First, a microscopic equilibrium description was specified in terms of discrete cavity modes populated according to Bose–Einstein statistics. Second, macroscopic equilibrium observables were constructed by aggregating these discrete contributions, yielding finite and well–behaved behavior in the absence of continuum assumptions. Third, frequency–resolved observables were examined, showing that a smooth Planck–like spectral envelope emerges naturally once finite boundary response and finite resolution cause neighboring equilibrium modes to overlap.

Taken together, these results show that the essential features of black–body radiation arise from the interplay of finite geometry, equilibrium statistics, and observability. The ultraviolet catastrophe is avoided not through the imposition of cutoffs or quantization postulates, but because unbounded continuum idealizations are never introduced. Planck's law is recovered as an effective macroscopic description valid in regimes where discrete geometric structure is dense relative to experimental resolution.

The scope of the present work is intentionally focused. Absolute normalization of the radiation spectrum, Wien displacement behavior, and Stefan–Boltzmann scaling are not derived here. These features require integration of the emergent spectral envelope and consideration of higher–dimensional geometric phase space beyond the finite–geometry, one–dimensional setting examined in this paper. Addressing these aspects constitutes the

natural continuation of the present analysis.

The broader significance of this result lies in its unifying character. Radiation, long regarded as a foundational exception necessitating the introduction of quantum postulates, is shown here to conform to the same finite–geometry principles that resolve divergences in fluid dynamics, gauge theory, magnetism, and gravitation within the Unified Lattice Framework. Equilibrium radiation is thereby placed on the same conceptual footing as other physical phenomena governed by bounded geometric structure.

Future work will extend the present framework to higher–dimensional cavities, derive thermodynamic radiation laws from the emergent spectral envelope, and explore the coupling of curvature–bounded radiation to gravitation and cosmological settings. These directions will further clarify the role of geometry as the organizing principle underlying equilibrium phenomena across physics.

Acknowledgments The author gratefully acknowledges the use of ChatGPT as an assistant for technical editing, reference verification, and clarity improvements during the preparation of this manuscript. All scientific concepts, geometric ideas, and theoretical developments presented in this work were formulated independently by the author.

References

1. William Hernandez. A Curvature–Bounded, Non–Singular Construction of Quantum Gravity. *Zenodo preprint*, 2025.
2. William Hernandez. Finite–Curvature Resolution of the Matter–Stability Problem: A Geometric Proof of Stability for Interacting Quantum Systems. *Zenodo preprint*, 2025.
3. William Hernandez. Navier–Stokes Existence and Smoothness from a Finite–Curvature Geometric Construction. *Zenodo preprint*, 2025.
4. William Hernandez. The Impartation Theorem for Curvature–Bounded Quantum Geometry. *Zenodo preprint*, 2025.
5. William Hernandez. The Magnetism Existence, Stability, and Emergence Problem: A Curvature–Bounded Derivation of Macroscopic Magnetization. *Zenodo preprint*, 2025.
6. William Hernandez. Unified Lattice Framework I: Geometric Resolutions of the Yang–Mills, Matter Stability, and Navier–Stokes Problems. *International Journal of Quantum Foundations*, 12(1):217–260, 2025.
7. William Hernandez. Unified Lattice Framework II: Curvature–Bound Resolutions of the Gravitational, Dark–Sector, and Singularity Problems. *International Journal of Quantum Foundations*, 12(1):261–335, 2025.
8. William Hernandez. Unified Lattice Framework III: Quantized Resolutions of the

Quantum–Gravity, Cosmogenic, and Continuity Problems. *International Journal of Quantum Foundations*, 12(1):336–363, 2025.

9. William Hernandez. Unified Lattice Framework Magnetism I-III: From Microscopic Coulomb Geometry to Curvature–Bounded Magnetic Operators and Macroscopic Phase Behavior. *Zenodo preprint*, 2025.
10. William Hernandez. Unified Lattice Framework: The Finite–Curvature Synthesis of Physics. *Zenodo preprint*, 2025.
11. William Hernandez. Yang–Mills Existence and Mass Gap from a Finite–Curvature Quantum Geometry. *Zenodo preprint*, 2025.